Exploring memory mechanisms for friction fatigue in vibratory pile driving

Tsetas, Athanasios; Tsouvalas, Apostolos; Metrikine, Andrei

DOI
10.1088/1742-6596/2767/6/062021

Publication date
2024

Document Version
Final published version

Published in
Journal of Physics: Conference Series

Citation (APA)
Tsetas, A., Tsouvalas, A., & Metrikine, A. (2024). Exploring memory mechanisms for friction fatigue in vibratory pile driving. *Journal of Physics: Conference Series*, *2767*(6), Article 062021. https://doi.org/10.1088/1742-6596/2767/6/062021

Journal of Physics: Conference Series

PAPER • **OPEN ACCESS**

Exploring memory mechanisms for friction fatigue in vibratory pile driving

To cite this article: Athanasios Tsetas *et al* 2024 *J. Phys.: Conf. Ser.* **2767** 062021

Exploring memory mechanisms for friction fatigue in vibratory pile driving

Athanasios Tsetas[1], **Apostolos Tsouvalas**[1], **Andrei Metrikine**[1]

[1]Faculty of Civil Engineering and Geosciences, Delft University of Technology, Stevinweg 1, Delft, 2628 CN, The Netherlands

E-mail: `a.tsetas@tudelft.nl`

Abstract. This paper studies the mechanism that leads to the reduction of frictional soil reaction forces during pile driving, termed friction fatigue. We focus on axial vibratory driving, an environmentally friendly monopile installation method, and examine two friction fatigue formulations, i.e. a penetration-based and a cyclic memory mechanism. Friction fatigue plays a pivotal role in pile drivability and post-installation bearing capacity for piles installed via axial vibratory driving. Through numerical analyses and validation against field data from onshore experiments, the efficacy of these memory mechanisms is assessed. The results reveal that the proposed cyclic memory mechanism provides consistently more accurate predictions than the corresponding penetration-based approach, offering a promising option for modelling friction fatigue in vibratory driving. This study advances our understanding of friction fatigue in the context of vibratory driving for offshore monopile installation, emphasizing the need for further numerical and experimental works in this topic.

1. Introduction

The installation of foundations for offshore wind turbines (OWTs) is a challenging operation during the construction of offshore wind farms. At present, the monopile concept comprises the majority of bottom-fixed OWT foundations globally, due to their simplicity and robustness compared to the other foundation options [1]. Furthermore, pile installation is also of interest to floating wind turbines deployed in deeper waters, where pile-type anchors are among the main foundation types [2]. These substructures are customarily tubular assemblages of cylindrical and conical segments, which are predominantly installed in the seabed by means of impact hammers [3]. The previous method is a robust technique, yet it generates high levels of underwater noise that pose a major environmental problem and have adverse effects on aquatic species [4]. As a response to this concern, alternative installation methods are increasingly gaining traction, with the offshore wind sector investigating the feasibility of more environmentally friendly solutions for monopile driving.

Vibratory driving is a well-known and established technique for installation of tubular and sheet piles, that is widely used in onshore construction projects [5, 6]. This installation technique is based on the application of axial excitation at the pile head - customarily via counter-rotating eccentric masses - forcing the pile into the ground and up to the target penetration depth. It is considered an efficient alternative to impact piling due to higher installation rates, lower pile stresses (and associated fatigue) and emitted noise. However, the limited experience with the vibro-driving method in offshore conditions requires significant efforts to address open research questions by means of numerical and experimental works. In the process of pile installation, the physical mechanism that leads to the reduction of soil friction along the shaft during driving is commonly termed "friction fatigue". Friction fatigue is a common concept among the different pile driving methods [7, 8, 9], yet the exact mechanism presumably differs among the various driving methods due to the dissimilar nature of the imposed soil stress state. In the case of vibratory driving, comprehension of friction fatigue is of major significance to quantify reliably the pile drivability and the post-installation bearing capacity [9]. Furthermore, we wish to bring attention to the concept of friction fatigue from another perspective, i.e. the underwater noise emissions during vibro-driving of offshore monopiles. In particular, the non-linear pile-soil coupling affects heavily the underwater noise field [10], thus rendering friction fatigue an essential component for its prediction.

The present paper explores potential mechanical descriptions that can capture the phenomenon of friction fatigue for the process of axial vibratory driving. In particular, a normalized penetration-based and a cyclic memory mechanism are formulated; their distinction is based on the state parameter that controls the rate of friction reduction, i.e. normalized penetration and number of loading cycles. The friction fatigue mechanism is applied to the pile-soil interface, which is based on Coulomb's friction. Furthermore, the vibro-driving model is comprised by a thin cylindrical shell and a linear elastic layered half-space coupled through the frictional interface and a non-linear tip reaction model [11]. Based on numerical analyses, the cyclic formulation presents a more favourable comparison with penetration measurements, showcasing its better suitability in qualitative and quantitative terms. The present model provides an effective engineering-oriented approach accounting for friction fatigue in vibro-driving and its formulation favours further development given the inflow of new experimental data.

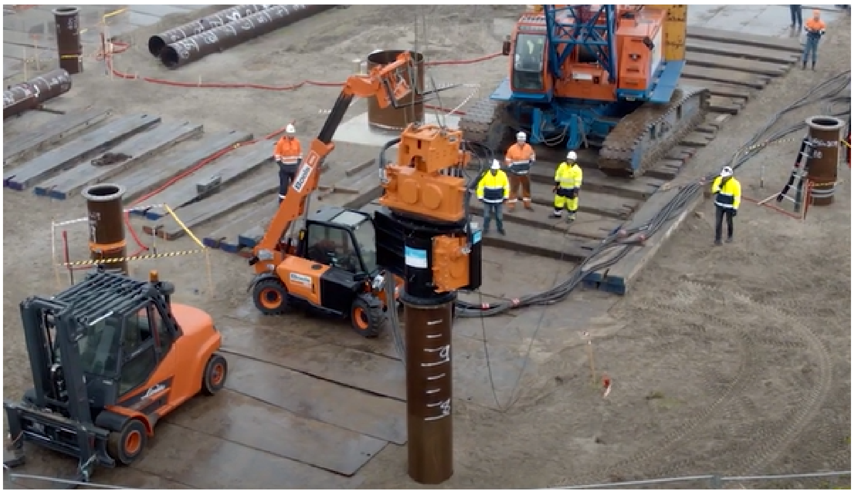

Figure 1: Medium-scale pile installation tests in an onshore sandy site.

2. Numerical modelling of vibratory pile driving

The description of the numerical model is presented in this section. Specifically, a modelling framework is employed, that is suitable for vibratory driving under axial and/or torsional excitation, thus addressing also a new pile installation technique termed "Gentle Driving of Piles" (GDP) [12]; the associated installation tests for model validation are shown in Fig. 1. Without further delay, the components of the preceding pile driving model (see Fig. 2) are as follows:

- a thin cylindrical shell based on the Love-Timoshenko theory [13, 14]; a semi-analytical finite element (SAFE) approach is used to model the cylindrical shell [11].
- a linear elastic layered half-space description is employed for the soil medium, modelled via the Thin-Layer Method (TLM) coupled with Perfectly Matched Layers (PMLs) to approximate the underlying half-space [15]. The Green's functions of this system are computed for ring sources in the frequency domain [16] and utilized in a hybrid frequency-time scheme based on the Harmonic Balance Method (HBM) [17].
- a CPT-based history-dependent non-linear interface between pile and soil along the shaft, based on Coulomb's friction law. A memory mechanism is incorporated that allows for the degradation of the friction amplitude as a function of a state parameter (described in Section 3) at a soil material point; this is an effective mechanism that accounts for the phenomenon of friction fatigue. Finally, a visco-elasto-plastic tip reaction model is used at the pile tip based on spring-dashpot values obtained from the 3-D soil continuum and plastic resistance characterized by the CPT measurements.

As regards the pile, a thin cylindrical shell is considered with wall thickness h_p, length L_p and mid-surface radius R_p based on the Love-Timoshenko theory. The shell material is linear isotropic elastic with Young's modulus E_p, Poisson's ratio ν_p and mass density ρ_p. Based on the SAFE method, the respective equations of motion read [11]:

$$\mathbf{I}_\mathrm{p}\frac{\mathrm{d}^2\mathbf{u}_\mathrm{p}}{\mathrm{d}t^2} + \mathbf{L}_\mathrm{p}\mathbf{u}_\mathrm{p} = \mathbf{p}_\mathrm{p} \tag{1}$$

where $\mathbf{I}_\mathrm{p}$ is the shell mass matrix, $\mathbf{L}_\mathrm{p}$ is the shell stiffness matrix, $\mathbf{u}_\mathrm{p}$ is the displacement/rotation vector and $\mathbf{p}_\mathrm{p}$ is the vector of consistent line forces/moments. It is remarked that the process of pile installation is considered axisymmetric. Furthermore, the line force/moment vector encompasses both the non-linear pile-soil interaction forces and the external input load. Finally, the pile displacement/rotation vector $\mathbf{u}_\mathrm{p}$ and the line force/moment vector $\mathbf{p}_\mathrm{p}$ read:

$$\mathbf{u}_\mathrm{p} = \begin{bmatrix} \mathbf{u} \\ \mathbf{w} \\ \boldsymbol{\beta}_z \end{bmatrix}, \quad \mathbf{p}_\mathrm{p} = \frac{1}{2\pi R_\mathrm{p}}\begin{bmatrix} \mathbf{p}_{z,\mathrm{p}} \\ \mathbf{p}_{r,\mathrm{p}} \\ \mathbf{m}_{zz,\mathrm{p}} \end{bmatrix} \tag{2}$$

The soil medium is considered a linear elastic layered half-space and modelled via the TLM+PMLs. By means of this approach, the Green's functions for ring sources are computed in the frequency-space domain and expressed as follows [18]:

$$\widetilde{\mathbf{u}}_\mathrm{s} = \begin{bmatrix} \widetilde{\mathbf{u}}_{r,\mathrm{s}} \\ \widetilde{\mathbf{u}}_{z,\mathrm{s}} \end{bmatrix} = \begin{bmatrix} \widetilde{\mathbf{F}}_{rr} & \widetilde{\mathbf{F}}_{rz} \\ \widetilde{\mathbf{F}}_{zr} & \widetilde{\mathbf{F}}_{zz} \end{bmatrix}\begin{bmatrix} \widetilde{\mathbf{p}}_{r,\mathrm{s}} \\ \widetilde{\mathbf{p}}_{z,\mathrm{s}} \end{bmatrix} \tag{3}$$

where $\widetilde{\mathbf{u}}_{r,\mathrm{s}}$, $\widetilde{\mathbf{u}}_{z,\mathrm{s}}$ are the vectors of soil displacements and $\widetilde{\mathbf{p}}_{r,\mathrm{s}}$, $\widetilde{\mathbf{p}}_{z,\mathrm{s}}$ are the vectors of ring loads in the indicated directions. The dynamic flexibility matrix is comprised by the sub-matrices $\widetilde{\mathbf{F}}_{rr}$, $\widetilde{\mathbf{F}}_{rz}$, $\widetilde{\mathbf{F}}_{zr}$ and $\widetilde{\mathbf{F}}_{zz}$ in the frequency-space domain.

The pile-soil coupling is realized through compatibility of applied tractions between pile and soil in all directions and continuity of radial displacements only; the vertical displacements of pile and soil differ such that sliding and thus pile penetration can be achieved. The shaft friction is described according to a history-dependent Coulomb friction model. In particular, a hyperbolic tangent regularization of Coulomb friction is employed for computational purposes [19]:

$$p_{z,\mathrm{s}}^{(i)} = -p_{z,\mathrm{p}}^{(i)} = f_{\mathrm{s,ult}}^{(i)} l^{(i)} \tanh\left(\frac{1}{v_\mathrm{tol}}\left(\frac{\partial u_\mathrm{p}^{(i)}}{\partial t} - \left.\frac{\partial u_{z,\mathrm{s}}^{(i)}}{\partial t}\right|_{r=R_\mathrm{p}}\right)\right) \tag{4}$$

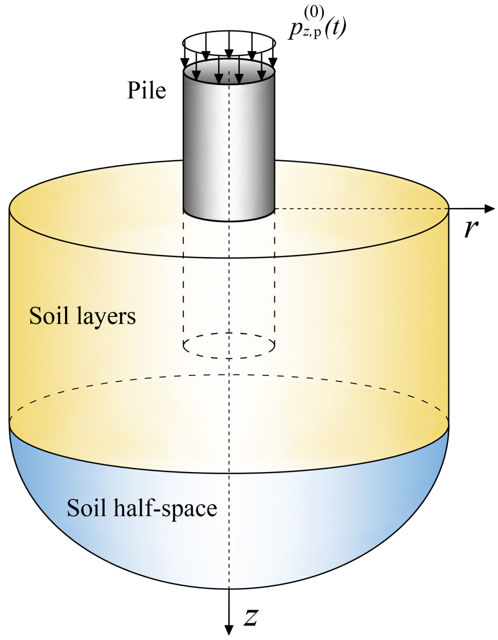

Figure 2: Model of a tubular pile installation in a layered soil medium via axial vibratory driving.

where v_{tol} denotes a velocity tolerance parameter, $l^{(i)}$ is the influence length obtained from the finite element projection and $f_{\mathrm{s,ult}}^{(i)}$ is the amplitude of the static (and kinetic) friction. The pile-soil coupling is completed with the tip reaction, which is expressed as:

$$p_{z,\mathrm{s}}^{(\mathrm{t})} = -p_{z,\mathrm{p}}^{(\mathrm{t})} = \begin{cases} k_{\mathrm{t}}(u_{\mathrm{p}}^{(\mathrm{t})} - u_{\mathrm{pl}}) + c_{\mathrm{t}} \dfrac{\partial u_{\mathrm{p}}^{(\mathrm{t})}}{\partial t}, & |k_{\mathrm{t}}(u_{\mathrm{p}}^{(\mathrm{t})} - u_{\mathrm{pl}})| < f_{\mathrm{t,ult}} h_{\mathrm{p}} \\ f_{\mathrm{t,ult}} h_{\mathrm{p}} \operatorname{sgn}\left(\dfrac{\partial u_{\mathrm{p}}^{(\mathrm{t})}}{\partial t}\right) + c_{\mathrm{t}} \dfrac{\partial u_{\mathrm{p}}^{(\mathrm{t})}}{\partial t}, & |k_{\mathrm{t}}(u_{\mathrm{p}}^{(\mathrm{t})} - u_{\mathrm{pl}})| = f_{\mathrm{t,ult}} h_{\mathrm{p}} \end{cases} \tag{5}$$

where u_{pl} is the plastic tip displacement, $f_{\mathrm{t,ult}}$ is the plastic tip resistance, whereas the stiffness and damping coefficients are defined as k_{t} and c_{t}, respectively. These coefficients are extracted from the soil dynamic stiffness matrix $\widetilde{\mathbf{K}}_{\mathrm{s}}$, obtained via inversion of the flexibility matrix $\widetilde{\mathbf{F}}_{\mathrm{s}}$.

Finally, the numerical solution of the full problem is obtained by means of sequential application of the Alternating Frequency-Time (AFT) Harmonic Balance Method (HBM) [20]. A more detailed description of the numerical solution method - as well as of the complete modelling framework - is given in [11] and will be omitted for the sake of brevity.

3. Friction fatigue modelling in vibratory pile driving via a memory mechanism

The gradual decrease of the ultimate shaft friction at a fixed (spatially) soil material point is occurring during different pile driving methods and is not met solely in vibratory installation. Heerema [7] observed that pile progression was accompanied by shaft friction reduction during impact piling tests in clay and termed this phenomenon "friction fatigue". Subsequently, a mechanism was proposed to describe friction fatigue based on the distance between the pile tip and the considered soil horizon, whereas the phenomenon was attributed to the decrease of horizontal soil stresses [7]. The reduction of radial effective stresses was also reported during jacking experiments and the ratio h/R was identified as the control parameter[21, 22]; parameters h and R being the distance of a soil material point from the pile tip and the pile radius, respectively. Sheng et al. [23] also verified the h/R effect in pile jacking via advanced FE simulations and found that the radial stress decrease above the tip level due to soil softening around the pile. Friction fatigue has been further considered in studies related to axial pile capacity [24, 25, 26].

Evidently, friction fatigue has received appreciable attention in various works related to pile foundations, yet there are limited studies and field observations on this topic in the context of vibratory driving. White and Lehane [8] conducted installation tests of centrifuge model piles including, among other techniques, a two-way cyclic jacked installation and its effect on the penetration process. It was found that shaft friction degradation had a better correlation with the number of cycles accumulated at a fixed soil material point than with the normalized distance from the tip (i.e. h/R). In a recent experimental campaign focused on vibratory pile installation tests, Moriyasu et al. [9] also reported findings that support this consideration, showing that the number of accumulated cycles is a more suitable control parameter than the h/R ratio. Based on the preceding findings, we proceed to formulate a history-dependent Coulomb friction law that accounts for shaft friction degradation, while retaining the number of state parameters as low as possible. To further investigate the plausibility of a normalized distance-based mechanism of friction reduction, the associated formulation reads as follows:

$$f_{\mathrm{s,ult}}^{(i)} = f_{\mathrm{s},0}^{(i)} \left(\beta_\infty + (1-\beta_\infty) \mathrm{e}^{-c_{\mathrm{D}} l_{\mathrm{D}}^{(i)}} \right) \tag{6}$$

where β_∞ is the ratio of the ultimately degraded friction amplitude to the initial one ($f_{\mathrm{s},0}^{(i)}$), $l_{\mathrm{D}}^{(i)}$ is the normalized distance of the soil interface (i) from the pile tip - normalized by the pile radius - and c_{D} is the memory parameter that controls the rate of degradation. It is noted that a similar formulation has been proposed for the axial capacity of piles driven in sand by Randolph et al. [27]. As can be understood, this model can be applied to other installation methods as well, presumably with different values for the proposed parameters. However, this statement does not hold for the ensuing cyclic memory that is governed by the number of loading cycles, implying a dynamic installation method with harmonic/periodic input. Accordingly, the mathematical expression of the cyclic memory mechanism for friction fatigue reads:

$$f_{\mathrm{s,ult}}^{(i)} = f_{\mathrm{s},0}^{(i)} \left(\beta_\infty + (1-\beta_\infty) \mathrm{e}^{-c_N N_{\mathrm{cycl}}^{(i)}} \right) \tag{7}$$

whereas $f_{\mathrm{s},0}^{(i)}$ and β_∞ have the same definitions as in the case of the distance-based mechanism and c_N is a memory parameter that controls the rate of degradation based on the number of loading cycles $N_{\mathrm{cycl}}^{(i)}$ accumulated at the soil interface (i) during driving. Therefore, in both mechanisms pile penetration leads to reduction of the friction force at soil material points in contact with the pile, yet this reduction is governed by dissimilar state variables leading to quantitative as well as qualitative discrepancies as will be shown in the Section 4.

Naturally, the proposed memory mechanisms are effective mechanical models and additional parameter dependencies may be important for further model refinement, e.g. driving frequency, loading amplitude and specific soil properties. A combination of experimental and numerical studies is necessary to comprehend the physical mechanisms underlying this phenomenon and allow to formulate efficient models for engineering use.

4. Numerical results and field data

In this section, the numerical results for the two different friction fatigue mechanisms are compared against field data from a medium-scale onshore test campaign [28]. The properties of the tubular vibro-driven pile from the GDP field campaign are given in Table 1. The experimental site comprised very dense to medium-dense sand and the water table ranged between 3.5 m and 4.5 m below the ground surface. Furthermore, the soil properties were characterized by means of Seismic Cone Penetration Tests with pore water pressure measurements (SCPTu) up to a target depth of 10 m. The measured profiles of cone tip resistance (q_c), relative density (D_r) and shear wave velocity (c_S) are displayed in Fig. 3. Regarding the input excitation, the axial input load is inferred from strain measurements recorded during installation via fiber Bragg grating (FBG) sensors at the pile head and is distributed uniformly along the circumference (see Fig. 4). It is remarked that the fundamental driving frequency was equal to $f = 24.8$ Hz. Finally, frequency-independent hysteretic damping is considered for both pile and soil in numerical analyses, with ratios $\xi_\mathrm{p} = 0.001$ and $\xi_\mathrm{s} = 0.025$ (identical for P- and S-waves), respectively.

Table 1: Properties of the vibro-driven pile.

E_p [Pa]	ν_p [-]	ρ_p [kg/m^3]	L_p [m]	R_p [m]	h_p [m]
$210{\cdot}10^9$	0.3	7850	10	0.373	0.0159

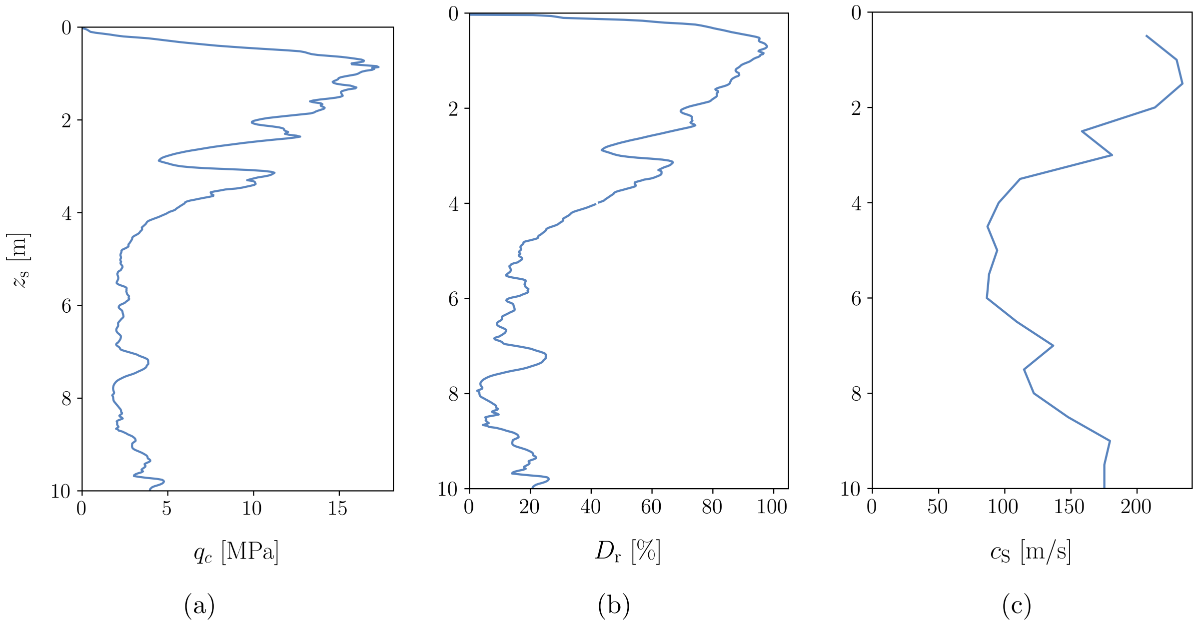

Figure 3: Profile of (a) cone tip resistance (q_c), (b) relative density (D_r), and (c) shear wave velocity (c_S) obtained from the SCPTu's.

In Fig. 5, the penetration predictions for the cyclic memory model are presented next to the penetration measurements; the latter are measured by two different set-ups, i.e. a potentiometer (PM) and a manual logging system (DL). As can be seen, the best match with the field data is found for $c_N = 0.0004$. However, it is noted that the other two predictions are also of added value, as they provide an upper and a lower bound and also follow qualitatively the penetration profile to a large extent. On the other hand, the predictions for the case of distance-based memory mechanism are shown in Fig. 6. It is apparent that the penetration profiles are not as accurate compared to the cyclic mechanism; for c_D values outside the present range the deviation was found to be even larger. Furthermore, another observation is that the predictions

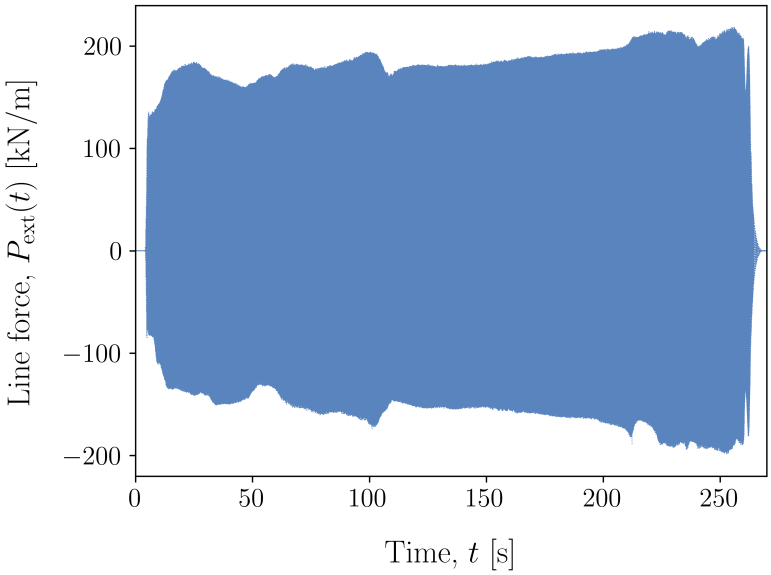

Figure 4: Axial line force inferred from the FBG strain measurements at the pile head.

provided in this case deviate from the measured penetration profile not only quantitatively, but also in qualitative terms. To summarize these results, the mean absolute error (MAE) of the penetration rate is provided in Table 2, showcasing that the cyclic formulation leads consistently to more reliable predictions than the normalized distance-based mechanism.

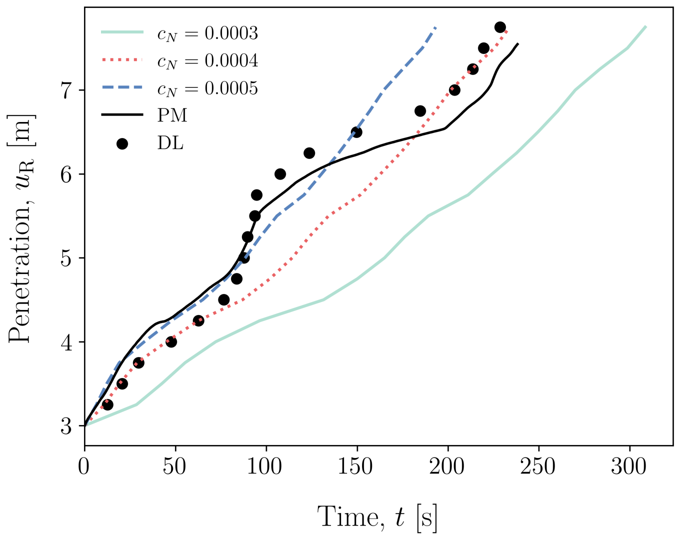

Figure 5: Comparison of vibratory installation model predictions with cyclic memory mechanism against penetration data measured by a potentiometer (PM) and the driving logging system (DL).

Overall, the cyclic memory mechanism (Fig. 5) leads to more accurate results in both quantitative and qualitative terms, whereas the normalized distance-based mechanism (Fig. 6) contradicts the field observations by predicting a monotonically increasing penetration rate. The cyclic mechanism appears more suitable, as it also provides upper and lower bound predictions,

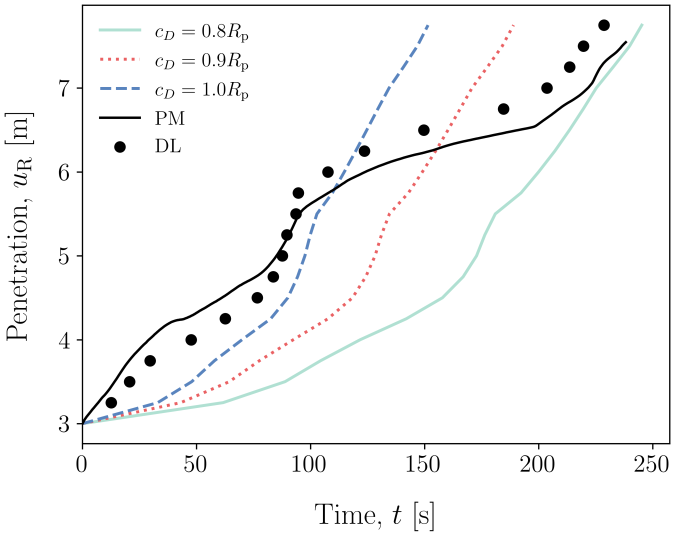

Figure 6: Comparison of vibratory installation model predictions with normalized distance-based memory mechanism against penetration data measured by a potentiometer (PM) and the driving logging system (DL).

Table 2: Mean absolute error (MAE) of penetration rate for the different memory mechanisms and control parameters.

	$c_N = 3 \cdot 10^{-4}$	$c_N = 4 \cdot 10^{-4}$	$c_N = 5 \cdot 10^{-4}$	$c_D = 0.8R_p$	$c_D = 0.9R_p$	$c_D = R_p$
MAE [mm/s]	11.65	10.72	12.72	17.27	25.05	28.19

thus being advantageous for engineering design purposes. It is remarked that similar results and strong correlation of friction fatigue with loading cycles has been found in pseudo-dynamic installation tests of centrifuge model piles by [8]. The body of observations for vibratory-driven piles is still scarce, so additional field data are necessary to consider such findings conclusive. Naturally, the inflow of field data from future experiments will serve to further refine our approach and to build the confidence needed for an engineering design. Finally, it is remarked that the presented model has been validated against field data from onshore tests in a sandy soil site with an upper unsaturated soil layer. Therefore, potential discrepancies from fully water-saturated conditions - met in the offshore environment - may be expected, pointing towards calibration refinement of the model with offshore driving data.

5. Conclusions

In this paper, a memory-enhanced frictional interface to account for friction fatigue in vibratory driving has been investigated. In particular, penetration-based and cyclic memory mechanisms have been formulated and compared against field data from a vibratory-driven pile. The former mechanism originates in impact hammering and pile jacking, thus it possesses little to no information about the dynamics of the process. The comparison between the numerical results and the field data indicates that such a mechanism leads to inadequate predictions both quantitatively and qualitatively. Conclusively, the proposed cyclic mechanism presents consistently more accurate results, forming lower and upper prediction bounds and showcasing its promising potential for use in engineering practice.

Acknowledgments
This research is associated with the GDP project in the framework of the GROW joint research program. Funding from "Topsector Energiesubsidie van het Ministerie van Econsomische Zaken" under grant number TE-HE117100 and financial/technical support from the following partners is gratefully acknowledged: Royal Boskalis Westminster N.V., CAPE Holland B.V., Deltares, Delft Offshore Turbine B.V., Delft University of Technology, ECN, Eneco Wind B.V., IHC IQIP B.V., RWE Offshore Wind Netherlands B.V., SHL Offshore Contractors B.V., Shell Global Solutions International B.V., Sif Netherlands B.V., TNO, and Van Oord Offshore Wind Projects B.V.

References

[1] Musial W, Spitsen P, Duffy P, Beiter P, Shields M, Hernando D M, Hammond R, Marquis M, King J and Sathish S 2023 Offshore Wind Market Report: 2023 Edition Tech. rep. National Renewable Energy Lab.(NREL), Golden, CO (United States)

[2] Cerfontaine B, White D, Kwa K, Gourvenec S, Knappett J and Brown M 2023 *Ocean Engineering* **279** 114327

[3] Jiang Z 2021 *Renewable and Sustainable Energy Reviews* **139** 110576

[4] Tsouvalas A 2020 *Energies* **13** 3037

[5] Whenham V and Holeyman A 2012 *Geotechnical and Geological Engineering* **30** 1119–1135

[6] Rainer Massarsch K, Wersäll C and Fellenius B H 2022 *Proceedings of the Institution of Civil Engineers-Geotechnical Engineering* **175** 31–48

[7] Heerema E P 1978 Predicting pile driveability: heather as an illustration of the friction fatigue theory *SPE european petroleum conference* (OnePetro)

[8] White D and Lehane B 2004 *Géotechnique* **54** 645–658

[9] Moriyasu S, Kobayashi S and Matsumoto T 2018 *Soils and foundations* **58** 853–865

[10] Molenkamp T, Tsetas A, Tsouvalas A and Metrikine A 2024 *Journal of Sound and Vibration* **576** 118298

[11] Tsetas A, Tsouvalas A and Metrikine A V 2023 *International Journal of Solids and Structures* **269** 112202

[12] Tsetas A, Tsouvalas A and Metrikine A V 2023 *International Journal of Solids and Structures* **282** 112466

[13] Love A E H 1944 *A treatise on the mathematical theory of elasticity* (Dover Publications)

[14] Timoshenko S P and Woinowsky-Krieger S 1959 *Theory of plates and shells* (McGraw-hill)

[15] de Oliveira Barbosa J M, Park J and Kausel E 2012 *Computer Methods in Applied Mechanics and Engineering* **217** 262–274

[16] Kausel E 1999 *International Journal of Solids and Structures* **36** 4725–4742

[17] Krack M and Gross J 2019 *Harmonic balance for nonlinear vibration problems* vol 1 (Springer)

[18] Kausel E and Peek R 1982 *Bulletin of the Seismological Society of America* **72** 1459–1481

[19] Marques F, Flores P, Claro J P and Lankarani H M 2016 *Nonlinear Dynamics* **86** 1407–1443

[20] Cameron T and Griffin J H 1989 *Journal of Applied Mechanics* **56** 149—-154

[21] Bond A and Jardine R 1991 *Geotechnique* **41** 341–363

[22] Lehane B M, Jardine R, Bond A J and Frank R 1993 *Journal of Geotechnical Engineering* **119** 19–35

[23] Sheng D, Eigenbrod K D and Wriggers P 2005 *Computers and Geotechnics* **32** 17–26

[24] Jardine R, Chow F, Overy R and Standing J 2005 *ICP design methods for driven piles in sands and clays* vol 112 (Thomas Telford London)

[25] Lehane B, Schneider J and Xu X 2005 *Frontiers in offshore geotechnics: ISFOG* 683–689

[26] Gavin K G and O'Kelly B C 2007 *Journal of Geotechnical and Geoenvironmental Engineering* **133** 63–71

[27] Randolph M, Dolwin R and Beck R 1994 *Geotechnique* **44** 427–448

[28] Tsetas A, Tsouvalas A, Gómez S, Pisanò F, Kementzetzidis E, Molenkamp T, Elkadi A and Metrikine A 2023 *Ocean Engineering* **270** 113453